JASS 2009 / Joint Advanced Student School / Saint Petersburg / March 29th – April 7th 2009
Course 3: Numerical Simulation in Turbomachinery

Simulation of Condensing Compressible Flows

Wendenburg, M.
Technische Universität München
Lehrstuhl für Fluidmechanik – Fachgebiet Gasdynamik
D-85747 Garching
GERMANY

Content

1 Introduction
2 Fundamentals
3 Modeling
4 Simulation
5 Conclusion

Abstract
This article gives a short introduction into the aspects of the simulation of compressible flows with condensation phenomena. The basic physical aspects are presented as well as a mathematical model describing them. Finally, the results of the implementation of the model into the Finite Volume Method (FVM) solver CATUM are presented.

Symbols used

Latin letters

a	Speed of sound
E	Spec. energy
e	Spec. internal energy
f	Frequency
g	Condensate mass fraction
J	Nucleation rate
m_v	Mass of a water vapor molecule
n	Number density of droplets
p	Pressure
p_i	Partial pressure of i
$p_{s,\infty}$	Vapor pressure
p_v	Partial pressure of vapor
R_i	Spec. gas constant for i
S	Supersaturation
T	Temperature
t	Time
u	Velocity
κ	Adiabatic exponent
ρ	Density
ρ_l	Density of liquid water
ρ_v	Partial density of water vapor
σ	Surface tension
Φ	Relative Humidity

Indices

0	at stagnation
v	vapor

1 Introduction

Compressible flows with condensation are observed for a large variety of applications. For example, design and optimization of thermal power plants enforce deep insight into the flow dynamics arising within steam turbines. Here, one observes the effects of condensation occurring in transonic flows of moist air or steam [1-3, 6, 9]. The presence of condensate is known to cause erosive effects due to impacting droplets on the surfaces of the blades. Furthermore, self excited oscillation leads to highly unsteady load as well as unsteady operating conditions of the turbine. Also, condensation leads to noticeable change in lift and drag of airfoils, such as airplane wings, and to losses in compression ratio in supersonic compressors as used in military jet fighters, too. Hence, the knowledge about these effects and how to deal with them is crucial especially during design stage.

2 Fundamentals

At low expansion speeds and hence low cooling rates phase transition of vapor or vapor/carrier gas mixtures from the gaseous to the liquid phase occurs close to equilibrium conditions because the time scales of the flow are far beyond the time scale of the phase transition process, for example during the formation of clouds.

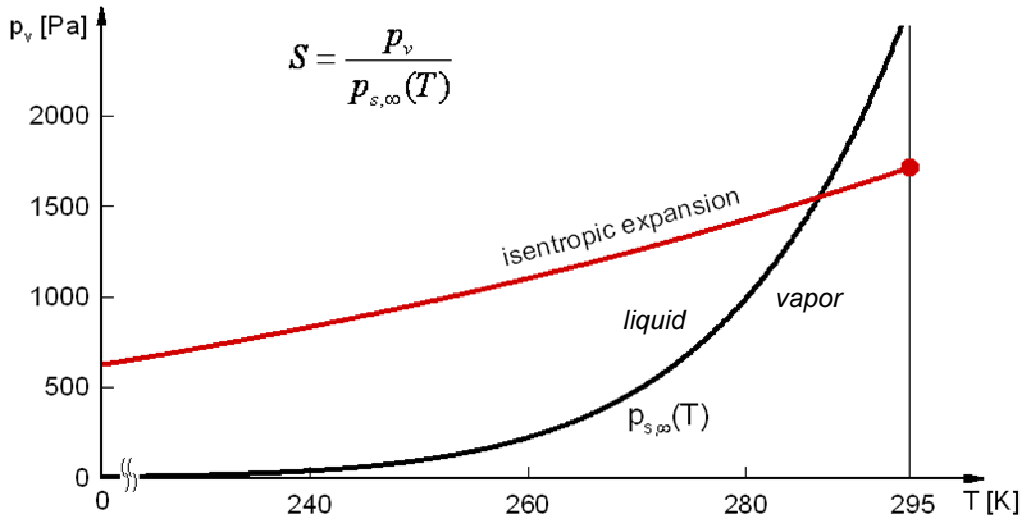

Figure 1: Isentropic expansion, beginning from T_0 = 295 K

But within transonic flows, which are compressible and have cooling rates of $\Delta T/\Delta t \approx 10^7$ K/s, non-equilibrium condensation effects play a major role as the time scale of advection is smaller than the time scale of the phase transition, which leads to subcooled vapor as sketched in Fig. 1 (red line). Now, nucleation and droplet growth become significant and drive the meta-stable thermodynamic state towards the saturation line (stable equilibrium state). Thereby, the release of the latent heat occurs nearly instantaneous and leads to a significant alternation of the flow field due to the increase of temperature.

Depending on stagnation conditions, different effects may occour in a certain geometry, and their complexity increases especially with stagnation humidity Φ_0:

- Continuous change in density, pressure etc.
  (in 1D: like geometry alteration)
- Discontinuous changes (shocks)
- Unsteady effects (oscillations)
- Unsymmetric, unsteady effects

Φ_0

With increasing Φ_0 the condensation onset shifts towards the area of critical mass flux while the amount of released latent heat increases. This leads to a discontinuous

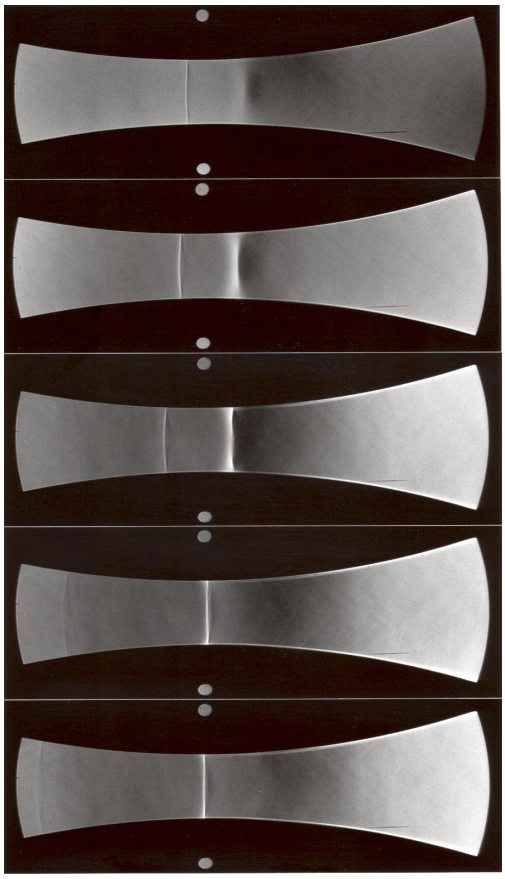

Figure 2: Schlieren visualization of self excited shock oscillation in a Laval nozzle [6]. Dots indicate the nozzle throat; circular arc nozzle, total throat height 30mm.

flow with shocks once that Φ_0 exceeds a certain limit. Further increase of Φ_0 will cause transient, oscillating shock waves.

Fig. 2 depicts Schlieren visualizations of a transient Laval nozzle flow of moist air [6]. The grey scale corresponds to the gradient of the density in axial direction, where lighter areas indicate compressions while darker areas are rarefractions. The five pictures show five instants in time of one complete cycle of a self excited shock oscillation with a frequency of f_{cycle} = 950 Hz. Starting with the first picture, due to the strong acceleration and the corresponding static pressure drop through the nozzle, the vapour phase reaches a meta-stable state shortly after the nozzle throat.

The release of latent heat caused by the onset of condensation causes a shock, displayed by the right bright line in the second picture. Here, the amount of heat released near the critical nozzle throat exceeds the possible amount of heat for a steady solution. Hence, the shock can not find a stable position and propagates upstream, even trough the nozzle throat (pictures 2-4). Thereby, the shock raises the temperature and the vapour phase behind the shock is no longer subcooled. Thus,

condensation disappears (picture 5). With the shock disappearing upstream and the re-offset of the condensation process, the flow again accelerates to a velocity where the vapour phase reaches a meta-stable state and the next cycle starts (picture 1).

Further increase of Φ_0 will finally provoke — at very high levels of Φ_0 — physical instabilities and make the oscillation unsymmetric. The goal of this work is to be able to simulate all those effects with one program.

3 Modeling

The effects of homogeneous condensation (nucleation and droplet growth) considered in this work were simulated with the finite volume solver **CATUM** (**C**ondens**a**tion **T**echnische **U**niversität **M**ünchen), which is a explicit, 1D/2D/3D structured multi-block grid solver for inviscid fluids based on a local Riemann Problem approach. The Equations to be solved are the Euler Equations and a equation of state required due to the compressible nature of the problem:

$$\frac{\partial \rho}{\partial t} + \nabla \cdot (\rho \vec{u}) = 0$$

$$\frac{\partial (\rho \vec{u})}{\partial t} + \nabla \cdot (\rho \vec{u} \otimes \vec{u} + p\underline{I}) = \vec{0}$$

$$\frac{\partial (\rho E)}{\partial t} + \nabla \cdot (\rho E \vec{u} + p\vec{u}) = 0$$

$$e = E - \tfrac{1}{2}\vec{u}^2$$

$$T = T(e, g_{\max}, g)$$

$$p = p(\rho, T, g_{\max}, g)$$

$$\kappa = \kappa(g_{\max}, g, T)$$

$$a = \sqrt{\kappa \tfrac{p}{\rho}}$$

and two transport equations for the condensate mass fraction g_{hom} as well as for the number density of droplets n_{hom}

$$\frac{\partial (\rho n_{\text{hom}})}{\partial t} + \nabla \cdot (\rho n_{\text{hom}} \vec{u}) = J_{\text{hom}}$$

$$\frac{\partial (\rho g_{\text{hom}})}{\partial t} + \nabla \cdot (\rho g_{\text{hom}} \vec{u}) = \left(\underbrace{\rho_l \tfrac{4\pi}{3} r^{*3} J_{\text{hom}}}_{\text{nucleation}} + \underbrace{\rho_l 4\pi \bar{r}_{\text{hom}}^2 \rho n_{\text{hom}} \frac{d\bar{r}_{\text{hom}}}{dt}}_{\text{droplet growth}} \right) .$$

The nucleation process is driven by the nucleation rate J_{hom} with

$$J_{\text{hom}} = \sqrt{\frac{2}{\pi} \cdot \frac{\sigma_\infty(T)}{m_v^3}} \cdot \frac{\rho_v^2}{\rho_l} \cdot \exp\left(-\frac{4\pi}{3} \cdot \frac{r_{\text{hom}}^{*2} \cdot \sigma_\infty(T)}{m_v \cdot R_v \cdot T} \right)$$

whereas the droplet growth follows the Hertz-Knudsen law

$$\frac{d\bar{r}_{\mathrm{hom}}}{dt} = \frac{\alpha}{\rho_l} \cdot \frac{p_v - p_{s,r}}{\sqrt{2\pi \cdot R_v \cdot T}}$$

With the absorption probability for water molecules $\alpha = 1$ and the vapor pressure for the curved droplet

$$p_{s,r} = p_{s,\infty}(T) \cdot \exp\left(\frac{2\sigma_\infty}{\rho_l \cdot R_v \cdot T \cdot r_{\mathrm{hom}}} \right) \quad .$$

The critical radius r^*_{hom} and the average droplet radius $\bar{r}_{\mathrm{hom}}$ are determined by

$$r^*_{\mathrm{hom}} = \frac{2\sigma_\infty}{\rho_l \cdot R_v \cdot T \cdot \ln(S)} \quad \text{and} \quad \bar{r}_{\mathrm{hom}} = \left(\frac{3}{4\pi} \cdot \frac{g}{\rho_l \cdot n_{\mathrm{hom}}} \right)^{\frac{1}{3}} \quad .$$

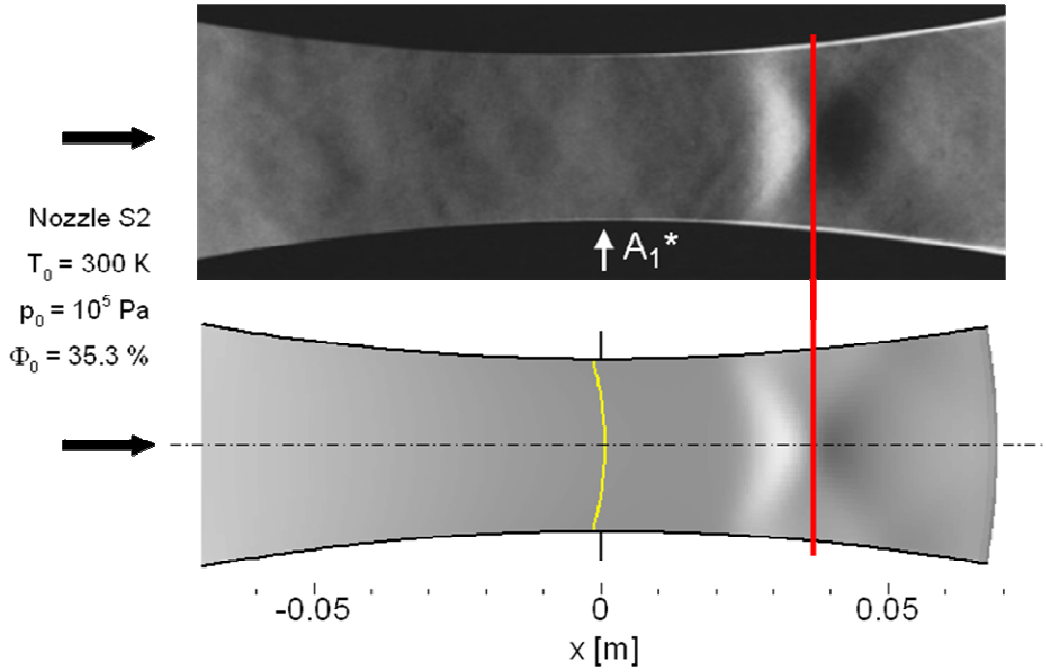

Figure 3: Comparison of Schlieren images for validation purposes

4 Simulation

For steady flows, the implementation was validated using known experimental test cases with available photographic Schlieren images which visualize the density gradient in direction of x. This optical method is suitable for comparisons due to ist high sensitivity to changes in the flow field.

As can be seen for the subcritical case in Fig. 3, e.g., the computed results match perfectly the experimental sample. The area of continuous compression is predicted correctly in both position and shape.

For unsteady flows the frequency of the oscillation was taken into account as well as numerical schlierem images to confirm the correctness of the simulation results. The frequencies obtained matched the values from experiments [1] precisely.

5 Conclusion

The simulation results obtained with the implemented model above show good results both in steady as well as in transient test cases. Hence, CATUM can now be considered to predict condensation effects accurately.

References

[1] Adam, S.: Numerische und experimentelle Untersuchung instationärer Düsenströmungen mit Energiezufuhr durch homogene Kondensation. PhD Thesis, Universität Karlsruhe (TH), 1996.
[2] Heiler, M.: Instationäre Phänomene in homogen/heterogen kondensierenden Düsen- und Turbinenströmungen. PhD Thesis, Universität Karlsruhe (TH), 1999.
[3] Mundinger, G.: Numerische Simulation instationärer Lavaldüsenströmungen mit Energiezufuhr durch homogene Kondensation. PhD Thesis, Universität Karlsruhe (TH), 1994.
[4] Schmidt, S.: Ein Verfahren zur präzisen Berechnung dreidimensionaler, reibungsfreier Idealgasströmungen über den gesamten Kompressibilitätsbereich. Diploma Thesis, Technische Universität München, 2005.
[5] Schnerr, G. H.: Gasdynamik, Lecture Notes. Technische Universität München, SS 2007.
[6] Schnerr, G. H.: Gasdynamische Strömungen mit Energiezufuhr und Phasenübergängen, Lecture Notes. Technische Universität München, WS 2007/08.
[7] Wagner, W. and Kretzschmar, H.-J.: International Steam Tables – Properties of Water and Steam Based on the Industrial Formulation IAPWS-IF97. Springer, Berlin Heidelberg, 2. Auflage, 2008.
[8] Wegener, P. P. and Mack, L. M.: Condensation in Supersonic and Hypersonic Wind Tunnels. In: von Kàrmàn, Th. and Dryden, H. L. (Editors): Advances in Applied Mechanics, Vol. V, p. 322. Academic Press Inc., New York, 1958.
[9] Winkler, G.: Laufrad-Leitrad-Wechselwirkung in homogen-heterogen konden-sierenden Turbinenströmungen. PhD Thesis, Universität Karlsruhe (TH), 2000.